Electronic Supplementary Information for

Discovery of a Highly Efficient Nitroaryl Group for Detection of Nitroreductase and Imaging of Hypoxic Tumor Cells

Shushu Wang,[†] Xiaojun Wu,[†] Yuqing Zhang, Dong Zhang, Boyu Xie, Zhixiang Pan, Kunfu Ouyang, Tao Peng*

State Key Laboratory of Chemical Oncogenomics, School of Chemical Biology and Biotechnology, Peking University Shenzhen Graduate School, Shenzhen 518055, China

[†]S. W. and X. W. contributed to this work equally.

*Correspondence: tpeng@pku.edu.cn

Table of Contents

Supplementary Figures

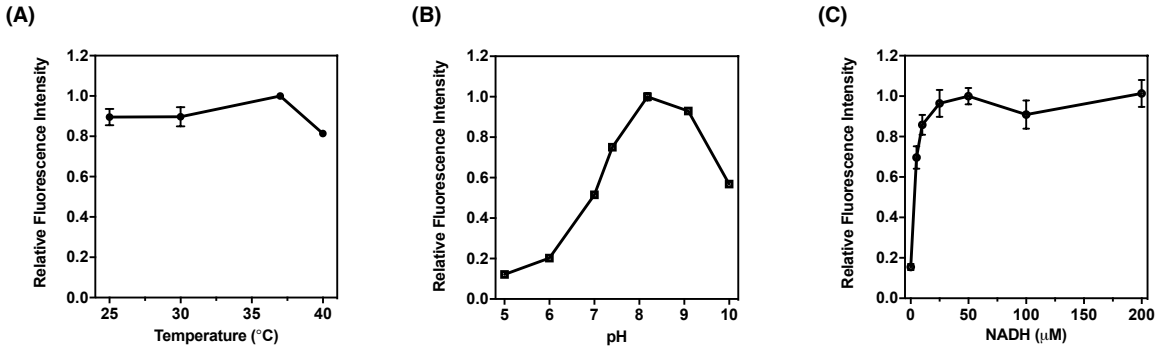

Figure S1. Photophysical characterization of NFP-7 for detection of NTR *in vitro*. (A) Fluorescence response of NFP-7 (10 μM) to NTR (1.0 μg/mL) in the presence of NADH (500 μM) at different temperatures in PBS (pH = 7.4). (B) Fluorescence response of NFP-7 (10 μM) to NTR (1.0 μg/mL) in the presence of NADH (500 μM) at different pH in PBS at 37 °C. (C) Fluorescence response of NFP-7 (10 μM) to NTR (1.0 μg/mL) in the presence of NADH at different concentrations pH in PBS (pH = 7.4) at 37 °C. NFP-7 was incubated with NTR in the presence of NADH at indicated temperature and pH for 30 min. The fluorescence intensities at 705 nm were recorded with excitation at 670 nm. Data are shown as mean ± standard deviation (*n* = 3).

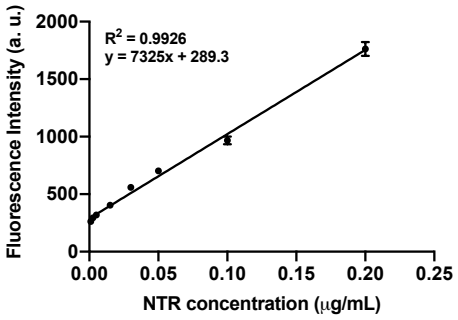

Figure S2. Linear relationship between NFP-7 fluorescence and NTR concentration and estimation of detection limit of NFP-7. NFP-7 (10 μM) was incubated with NTR at different concentrations in the presence of NADH (500 μM) in PBS (pH = 7.4) at 37 °C for 30 min. The fluorescence intensities at 705 nm were recorded with excitation at 670 nm. Data are shown as mean ± standard deviation (*n* = 3).

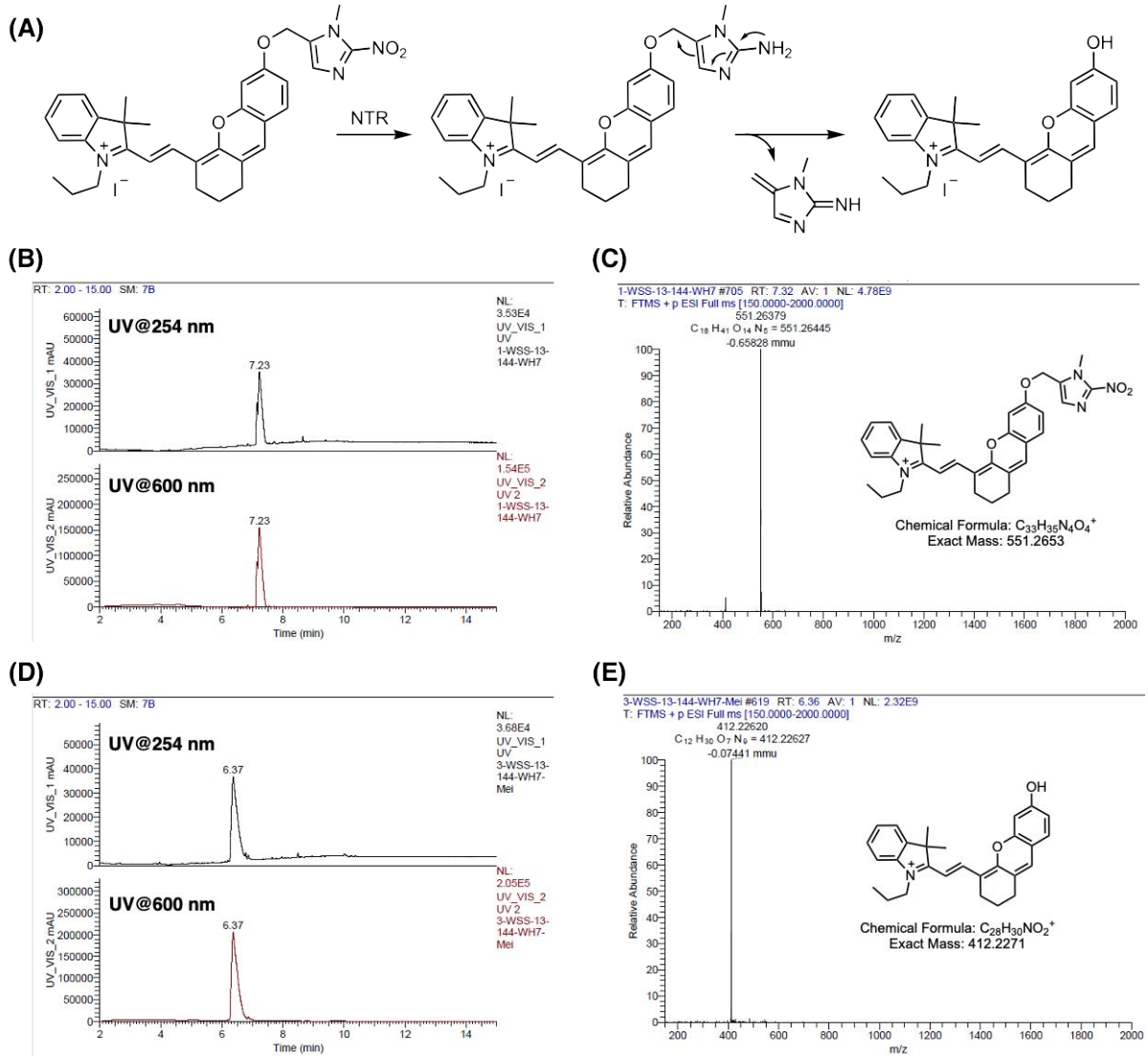

Figure S3. LC-MS analysis of the reaction between NFP-7 and NTR. NFP-7 (200 μM) was incubated with NTR (1.0 μg/mL) in the presence of NADH (1 mM) in PBS (pH = 7.4) at 37 °C for 5 min. The mixture was directly analyzed by LC-MS. (A) The reaction between NFP-7 and NTR generates the hemicyanine product. (B) LC traces of NFP-7 before reaction with NTR. (C) MS spectra at 7.23 min in (B) showing the presence of NFP-7. (D) LC traces of the reaction mixture between NFP-7 and NTR. (E) MS spectra at 6.37 min in (D) showing the presence of the hemicyanine product.

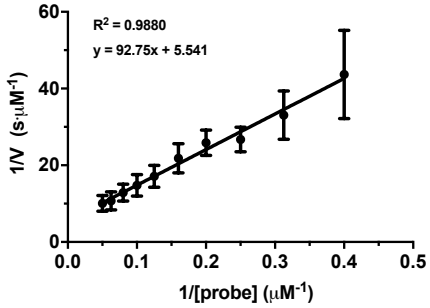

Figure S4. Determination of the enzymatic parameters for reaction between NTR and NFP-7 using the Lineweaver-Burk plot. The probe (2.5–20 μM) was incubated with NTR (0.1 μg/mL) in the presence of NADH (500 μM) in PBS (pH = 7.4) at 37 °C. The fluorescence intensities at 705 nm (excited at 670 nm) were monitored immediately after NTR addition with time increasing. The reaction at each probe concentration was repeated three times. Data are shown as mean ± standard deviation (n = 3). The Lineweaver-Burk equation was described as: $1/V = 1/V_{max} + K_m/V_{max} \cdot 1/[probe]$, where V is the initial reaction rate, [probe] is the probe concentration, K_m is the Michaelis constant, and V_{max} is the maximal reaction rate. K_m and V_{max} are thus calculated to be 16.7 μM and 0.18 μM s^{-1}, respectively.

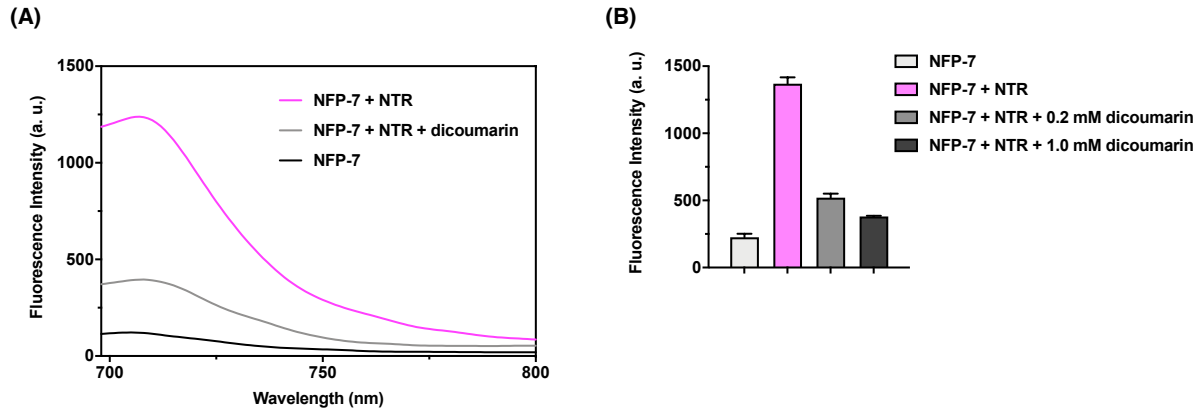

Figure S5. Addition of dicoumarin decreases the fluorescence response of NFP-7 to NTR. (A) Fluorescence spectra of NFP-7 (10 μM) before (black) and after (pink) incubation with NTR (1.0 μg/mL) in the absence (pink) or presence (gray) of dicoumarin (0.2 mM). (B) Fluorescence response of NFP-7 (10 μM) to NTR (1.0 μg/mL) in the absence or presence of dicoumarin (0.2 or 1.0 mM). NFP-7 (10 μM) was incubated with NTR (1.0 μg/mL) in the presence of NADH (500 μM) in PBS (pH = 7.4) at 37 °C for 30 min. The fluorescence intensities at 705 nm were recorded with excitation at 670 nm. Data are shown as mean ± standard deviation (n = 3).

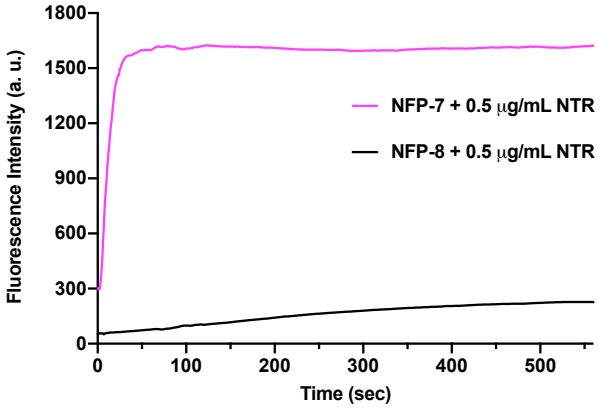

Figure S6. Comparison of NFP-7 (10 μM) and NFP-8 (10 μM) on absolute fluorescence responses and kinetics toward NTR (0.5 μg/mL) in the presence of NADH (500 μM) at 37 °C. NFP-7–8 were excited at 670 nm, and fluorescence intensities at 705 nm were monitored with time.

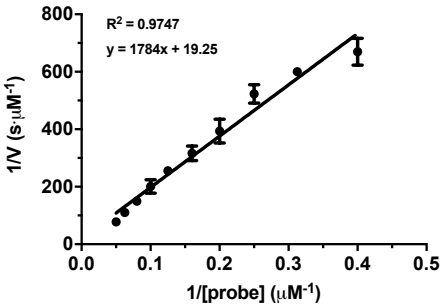

Figure S7. Determination of the enzymatic parameters for reaction between NTR and NFP-8 using the Lineweaver-Burk plot. The probe (2.5–20 μM) was incubated with NTR (1.0 μg/mL) in the presence of NADH (500 μM) in PBS (pH = 7.4) at 37 °C. The fluorescence intensities at 705 nm (excited at 670 nm) were monitored immediately after NTR addition with time increasing. The reaction at each probe concentration was repeated three times. Data are shown as mean ± standard deviation (n = 3). The Lineweaver-Burk equation was described as: $1/V = 1/V_{max} + K_m/V_{max} \cdot 1/[probe]$, where V is the initial reaction rate, [probe] is the probe concentration, K_m is the Michaelis constant, and V_{max} is the maximal reaction rate. K_m and V_{max} are thus calculated to be 92.7 μM and 0.052 μM s^{-1}, respectively.

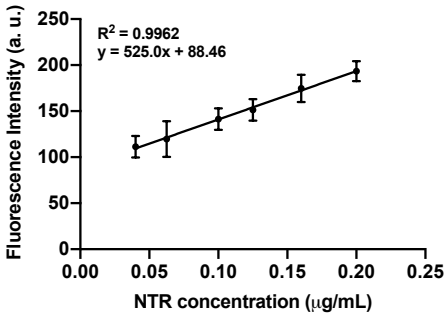

Figure S8. Linear relationship between NFP-8 fluorescence and NTR concentration and estimation of detection limit of NFP-8. NFP-8 (10 μM) was incubated with NTR at different concentrations in the presence of NADH (500 μM) in PBS (pH = 7.4) at 37 °C for 60 min. The fluorescence intensities at 705 nm were recorded with excitation at 670 nm. Data are shown as mean ± standard deviation (*n* = 3).

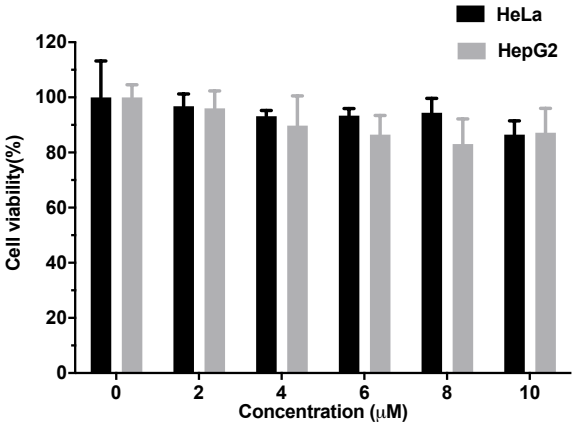

Figure S9. Cytotoxicity of NFP-7 in HeLa (black) and HepG2 (gray) cells. Cells were incubated with NFP-7 at corresponding concentrations for 12 h. Cell viability was measured by MTT assay and reported as percentage relative to untreated cells. Data are shown as mean ± standard deviation (*n* = 3).

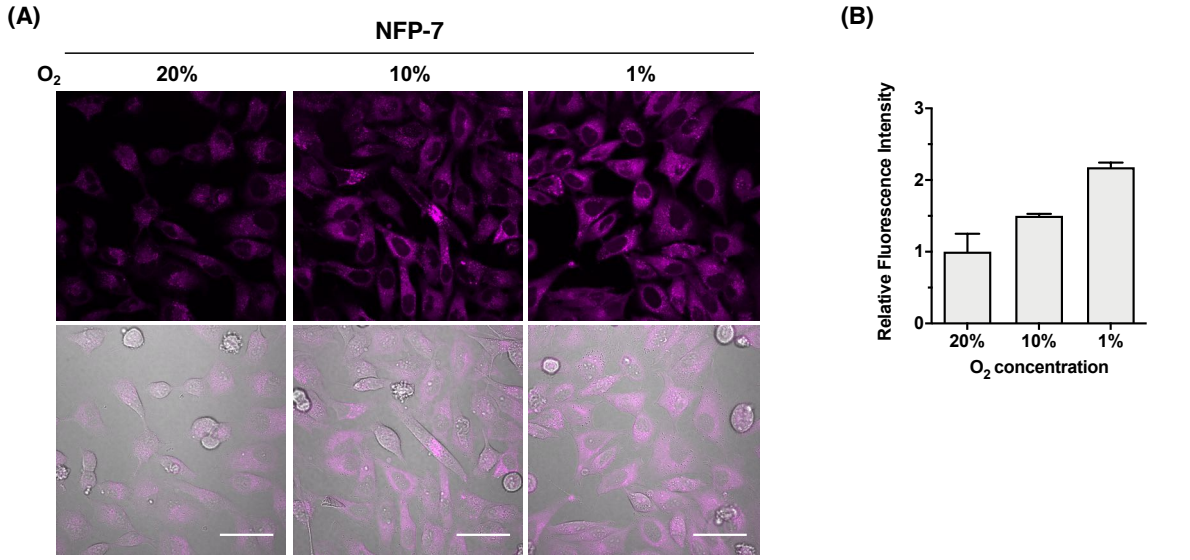

Figure S10. Confocal fluorescence imaging of HeLa cells with NFP-7 under hypoxic conditions. (A) Cells were incubated with NFP-7 (5 μM) under normoxic (20% O_2) or different hypoxia conditions (10% or 1% O_2) for 5 h, washed with PBS, and imaged by confocal fluorescence microscopy. The fluorescence signals of NFP-7 were collected between wavelengths of 663 and 738 nm, with excitation at 640 nm. Scale bars represent 50 μm. (B) Quantification of fluorescence images shown in (A). The y-axis represents fluorescence intensities of cells relative to those under normoxic conditions. Data are shown as mean relative fluorescence intensity ± standard deviation (*n* = 3 independent experiments).

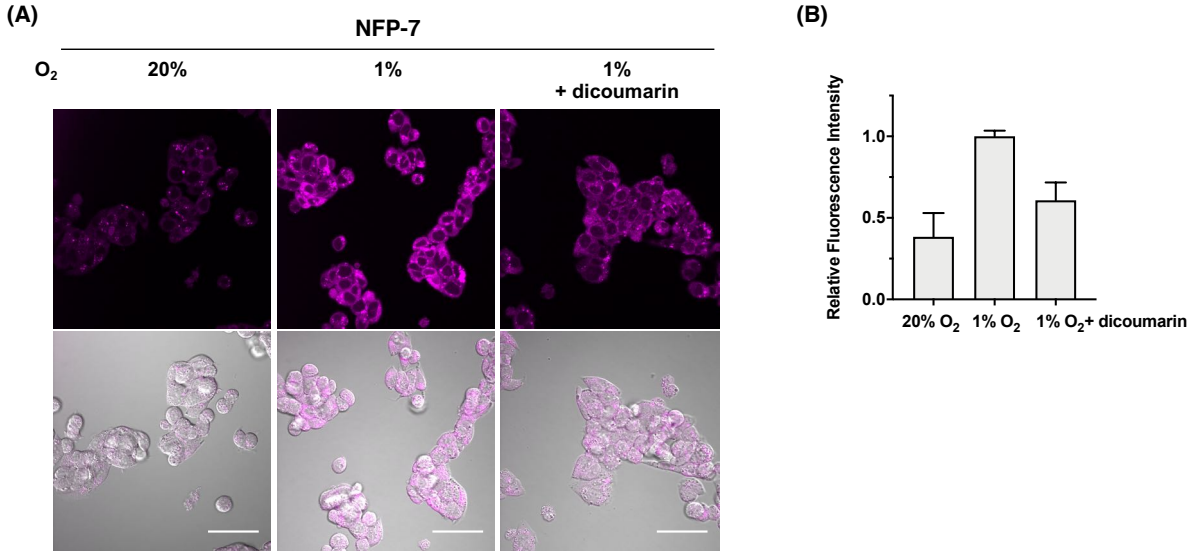

Figure S11. Confocal fluorescence imaging of HepG2 cells with NFP-7 under hypoxic conditions with dicoumarin treatment. (A) Cells were incubated with NFP-7 (5 μM) under normoxic (20% O_2) or hypoxic conditions (1% O_2) in the absence or presence of dicoumarin (0.2 mM) for 5 h, washed with PBS, and imaged by confocal fluorescence microscopy. The fluorescence signals of NFP-7 were collected between wavelengths of 663 and 738 nm, with

excitation at 640 nm. Scale bars represent 50 μm. (B) Quantification of fluorescence images shown in (A). The y-axis represents fluorescence intensities of cells relative to those under normoxic conditions. Data are shown as mean relative fluorescence intensity ± standard deviation (*n* = 3 independent experiments).

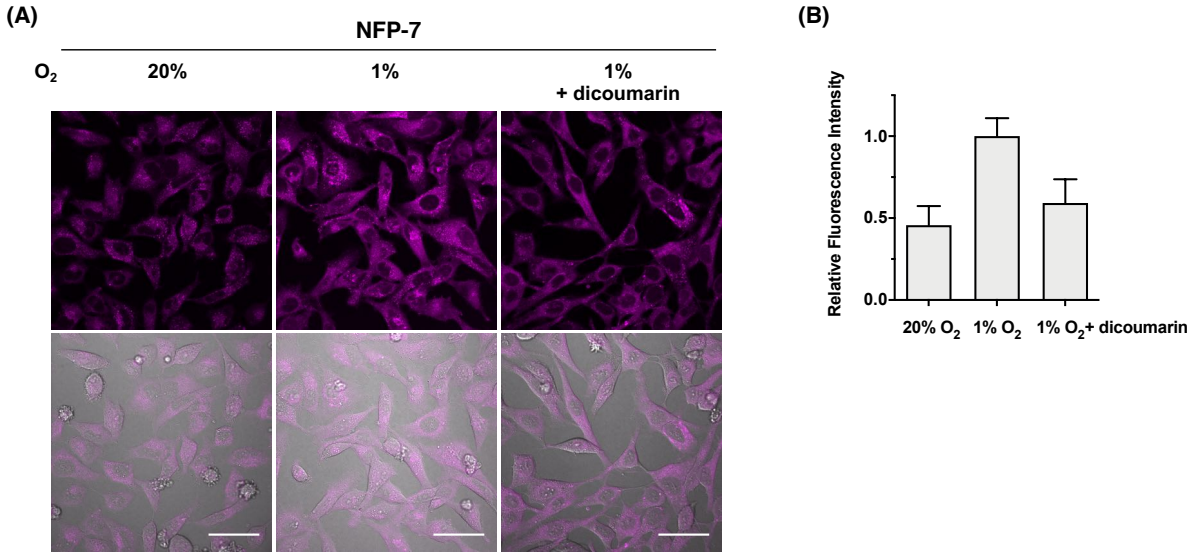

Figure S12. Confocal fluorescence imaging of HeLa cells with NFP-7 under hypoxic conditions with dicoumarin treatment. (A) Cells were incubated with NFP-7 (5 μM) under normoxic (20% O_2) or hypoxic conditions (1% O_2) in the absence or presence of dicoumarin (0.2 mM) for 5 h, washed with PBS, and imaged by confocal fluorescence microscopy. The fluorescence signals of NFP-7 were collected between wavelengths of 663 and 738 nm, with excitation at 640 nm. Scale bars represent 50 μm. (B) Quantification of fluorescence images shown in (A). The y-axis represents fluorescence intensities of cells relative to those under normoxic conditions. Data are shown as mean relative fluorescence intensity ± standard deviation (*n* = 3 independent experiments).

Synthetic materials and methods

Commercially available chemicals were generally obtained from Sigma-Aldrich, Acros, or TCI, and used as received without further purification. Chemical reactions were performed in oven-dried flasks under a N_2 atmosphere when air- or moisture-sensitive reagents were used. Anhydrous tetrahydrofuran (THF) was distilled from sodium/benzophenone. Anhydrous dichloromethane (CH_2Cl_2) was distilled from calcium hydride. Anhydrous dimethylformamide (DMF) was purchased from Sigma-Aldrich. Analytical TLC was conducted on GF_{254} silica gel plates from Qingdao Haiyang Chemical Co., Ltd, and visualized by illumination with a 254 nm UV light and/or staining with iodine (I_2) or phosphomolybdic acid (PMA). Silica gel (230-400 mesh, reagent grade) for flash column chromatography was purchased from Qingdao Haiyang Chemical Co., Ltd. The ^1H and ^{13}C NMR spectra were recorded in $CDCl_3$ or CD_3OD at room temperature on a Bruker Avance-300 NMR Spectrometer operating at 300 MHz for ^1H, a Bruker Avance-400 NMR Spectrometer operating at 400 MHz for ^1H, or a Bruker Avance-500 NMR Spectrometer operating at 500 MHz for ^1H. Chemical shifts are reported in δ ppm, and J values are reported in Hz. ^1H NMR chemical shifts were reported using tetramethylsilane (TMS, δ = 0.00 ppm) in $CDCl_3$ or CD_3OD (CD_3, δ = 3.31 ppm) as the internal standard. ^{13}C NMR chemical shifts were reported using $CDCl_3$ (δ = 77.16 ppm) or CD_3OD (δ = 49.00 ppm) as the internal standard. Splitting patterns are shown as follows: br, broad; s, singlet; d, doublet; t, triplet; m, multiplet; dd, doublet of doublets; dt, doublet of triplets. High resolution ESI mass spectra were recorded with an ABI QSTAR Elite or Q Extractive Plus mass spectrometer. LC-MS analysis was performed on a Q Exactive Focus LC-MS/MS System.

Synthesis of resorufin-derived probes NFP-1–6

Resorufin-derived probes NFP-1–6 were synthesized according to Scheme S1.

Scheme S1. Synthesis of resorufin-derived probes NFP-1–6.

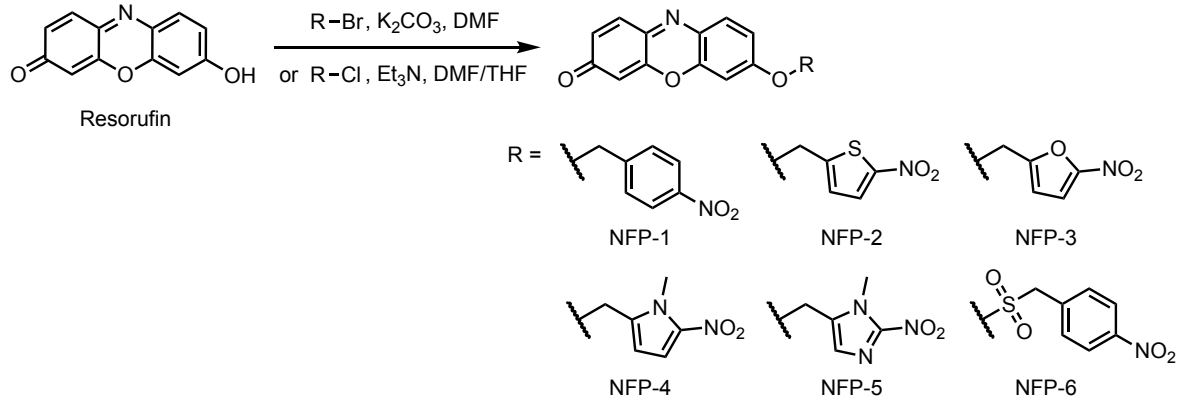

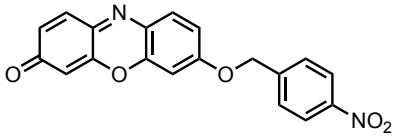

7-((4-nitrobenzyl)oxy)-3*H*-phenoxazin-3-one (NFP-1). To a solution of resorufin (63 mg, 0.3 mmol, 1.0 eq) in DMF (3 mL) were added K_2CO_3 (62 mg, 0.45 mmol, 1.5 eq) and 1-(bromomethyl)-4-nitrobenzene (64 mg, 0.3 mmol, 1.0 eq). The mixture was stirred at 40 °C for 2 h, then diluted with CH_2Cl_2 (20 mL), and washed with water (3 × 10 mL). The organic layer was dried over Na_2SO_4, filtered, and concentrated in vacuo. The resulting residue was

recrystallized with CH_2Cl_2 and hexane to yield NFP-1 (37 mg, 35%) as a red solid. ^{1}H NMR (300 MHz, $CDCl_3$ + 10% CF_3COOH) δ 8.42 – 8.30 (m, 3H), 8.24 (d, *J* = 9.5 Hz, 1H), 7.71 (d, *J* = 8.7 Hz, 2H), 7.62 (dd, *J* = 9.4, 2.4 Hz, 2H), 7.46 (d, *J* = 2.6 Hz, 1H), 7.44 (d, *J* = 2.6 Hz, 1H), 5.52 (s, 2H). HRMS calcd for $C_{19}H_{13}N_2O_5$ $[M+H]^+$ 349.0824, found 349.0819.

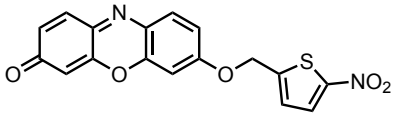

7-((5-nitrothiophen-2-yl)methoxy)-3*H*-phenoxazin-3-one (NFP-2). To a solution of resorufin (85 mg, 0.4 mmol, 1.0 eq) in DMF (3 mL) were added K_2CO_3 (82 mg, 0.6 mmol, 1.5 eq) and 2-(bromomethyl)-5-nitrothiophene (81 mg, 0.4 mmol, 1.0 eq). The mixture was stirred at 40 °C for 2 h, then diluted with CH_2Cl_2 (20 mL), and washed with water (3 × 10 mL). The organic layer was dried over Na_2SO_4, filtered, and concentrated in vacuo. The resulting residue was recrystallized with CH_2Cl_2 and hexane to yield NFP-2 (31 mg, 22%) as a red solid. ^{1}H NMR (300 MHz, $CDCl_3$ + 10% CF_3COOH) δ 8.13 (d, *J* = 9.3 Hz, 1H), 7.98 (d, *J* = 9.6 Hz, 1H), 7.77 (d, *J* = 2.4 Hz, 1H), 7.46 (dd, *J* = 9.3, 2.4 Hz, 1H), 7.39 (d, *J* = 4.2 Hz, 1H), 7.34 (dd, *J* = 9.7, 2.5 Hz, 1H), 7.26 (d, *J* = 2.5 Hz, 1H), 6.72 (d, *J* = 4.2 Hz, 1H), 5.27 (s, 2H). HRMS calcd for $C_{17}H_{11}N_2O_5S$ $[M+H]^+$ 355.0389, found 355.0383.

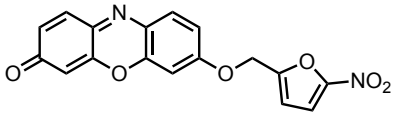

7-((5-nitrofuran-2-yl)methoxy)-3*H*-phenoxazin-3-one (NFP-3). To a solution of resorufin (42 mg, 0.2 mmol, 1.0 eq) in DMF (3 mL) were added K_2CO_3 (41 mg, 0.3 mmol, 1.5 eq) and 2-(bromomethyl)-5-nitrofuran (40 mg, 0.2 mmol, 1.0 eq). The mixture was stirred at 40 °C for 2 h, then diluted with CH_2Cl_2 (20 mL), and washed with water (3 × 10 mL). The organic layer was dried over Na_2SO_4, filtered, and concentrated in vacuo. The resulting residue was recrystallized with CH_2Cl_2 and hexane to yield NFP-3 (58 mg, 85%) as a red solid. ^{1}H NMR (300 MHz, $CDCl_3$ + 10% CF_3COOH) δ 8.34 (d, *J* = 9.3 Hz, 1H), 8.25 (d, *J* = 9.5 Hz, 1H), 7.63 (dd, *J* = 9.5, 2.2 Hz, 1H), 7.58 (dd, *J* = 9.3, 2.6 Hz, 1H), 7.50 (d, *J* = 2.6 Hz, 1H), 7.45 (d, *J* = 2.3 Hz, 1H), 7.40 (d, *J* = 3.7 Hz, 1H), 6.89 (d, *J* = 3.7 Hz, 1H), 5.43 (s, 2H). HRMS calcd for $C_{17}H_{11}N_2O_6$ $[M+H]^+$ 339.0617, found 339.0612.

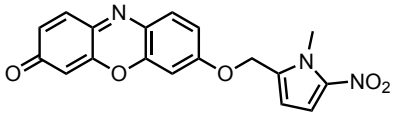

7-((1-methyl-5-nitro-1*H*-pyrrol-2-yl)methoxy)-3*H*-phenoxazin-3-one (NFP-4). To a solution of resorufin (74 mg, 0.35 mmol, 0.8 eq) in DMF (3 mL) were added K_2CO_3 (193 mg, 1.4 mmol, 4 eq) and 2-(bromomethyl)-1-methyl-5-nitro-1*H*-pyrrole[1] (94 mg, 0.43 mmol, 1.0 eq). The mixture was stirred at 40 °C for 2 h, then diluted with CH_2Cl_2 (20 mL), and washed with water (3 × 10 mL). The organic layer was dried over Na_2SO_4, filtered, and concentrated in vacuo. The resulting residue was recrystallized with CH_2Cl_2 and hexane to yield NFP-4 (16 mg, 13%) as a red solid. ^{1}H NMR (300 MHz, $CDCl_3$ + 10% CF_3COOH) δ 8.31 (d, *J* = 9.3 Hz, 2H), 7.68 (d, *J* = 1.9 Hz, 1H), 7.61 (dd, *J* = 9.4, 2.4 Hz, 2H), 7.49 (d, *J* = 2.5 Hz, 2H), 6.96 (d, *J* = 2.0 Hz, 1H), 5.33 (s, 2H), 3.77 (s, 3H). HRMS calcd for $C_{18}H_{14}N_3O_5$ $[M+H]^+$ 352.0933, found 352.0929.

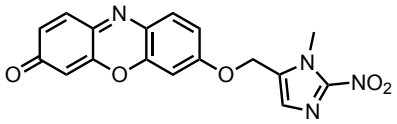

7-((1-methyl-2-nitro-1*H*-imidazol-5-yl)methoxy)-3*H*-phenoxazin-3-one (NFP-5). To a solution of resorufin (50 mg, 0.23 mmol, 1.0 eq) in DMF (3 mL) were added K_2CO_3 (47 mg, 0.34 mmol, 1.5 eq) and 5-(bromomethyl)-1-methyl-2-nitro-1H-imidazole[2-3] (52 mg, 0.23 mmol, 1.0 eq). The mixture was stirred at 40 °C for 2 h, then diluted with CH_2Cl_2 (20 mL), and washed with water (3 × 10 mL). The organic layer was dried over Na_2SO_4, filtered, and concentrated in vacuo. The resulting residue was recrystallized with CH_2Cl_2 and hexane to yield NFP-5 (38 mg, 46%) as a red solid. ^{1}H NMR (300 MHz, $CDCl_3$ + 10% CF_3COOH) δ 8.30 (d, *J* = 9.6 Hz, 1H), 8.19 (d, *J* = 9.6 Hz, 1H), 7.63 (s, 1H), 7.57 (dd, *J* = 9.5, 2.1 Hz, 1H), 7.50 – 7.48 (m, 2H), 7.36 (d, *J* = 2.3 Hz, 1H), 5.46 (s, 2H), 4.21 (s, 3H). HRMS calcd for $C_{17}H_{12}N_4O_5$ $[M+H]^+$ 353.0886, found 353.0839.

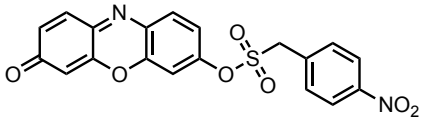

3-oxo-3*H*-phenoxazin-7-yl (4-nitrophenyl)methanesulfonate (NFP-6). To a solution of resorufin sodium salt (47 mg, 0.2 mmol, 1.0 eq) and Et_3N (0.05 mL, 0.4 mmol, 2.0 eq) in DMF (3 mL) was added the solution of (4-nitrophenyl)methanesulfonyl chloride (70 mg, 0.3 mmol, 1.5 eq) in THF(1 mL) dropwise at 0 °C. The mixture was stirred at room temperature for 1h, diluted with ethyl acetate (20 mL), and washed with water (3 × 10 mL). The organic layer was dried over Na_2SO_4, filtered, and concentrated in vacuo. The resulting residue was recrystallized by CH_2Cl_2 and hexane to yield NFP-6 (44 mg, 53%) as a red solid. ^{1}H NMR (500 MHz, $CDCl_3$ + 10% CF_3COOH) δ 8.34 (d, *J* = 8.3 Hz, 2H), 8.05 (d, *J* = 8.9 Hz, 1H), 7.76 (d, *J* = 9.8 Hz, 1H), 7.71 (d, *J* = 8.3 Hz, 2H), 7.37 (s, 1H), 7.31 (d, *J* = 8.9 Hz, 1H), 7.22 (d, *J* = 9.9 Hz, 1H), 6.74 (s, 1H), 4.78 (s, 2H). HRMS calcd for $C_{19}H_{13}N_2O_7S$ $[M+H]^+$ 413.0443, found 413.0437.

Synthesis of hemicyanine-derived probes NFP-7–8

Hemicyanine-derived probes NFP-7–8 were synthesized according to Scheme S2.

Scheme S2. Synthesis of probes NFP-7–8.

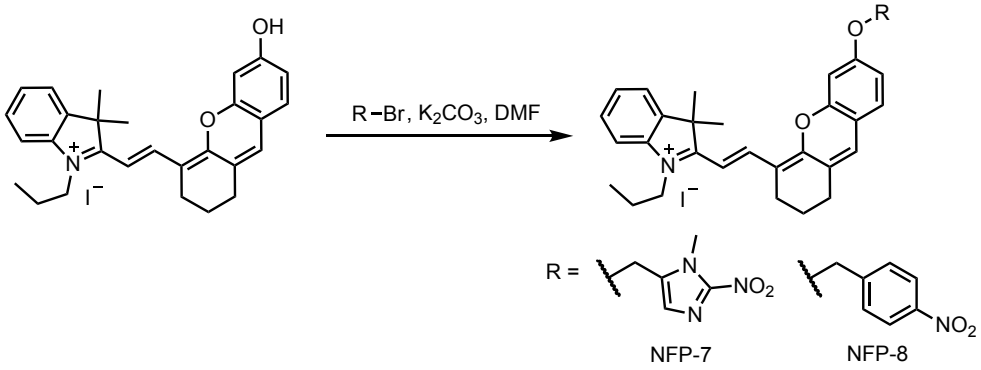

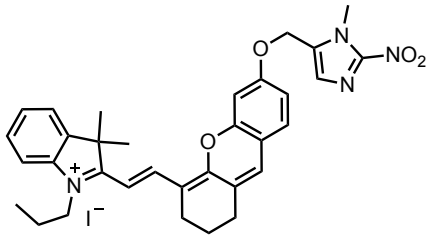

3,3-dimethyl-2-(2-(6-((1-methyl-2-nitro-1*H*-imidazol-5-yl)methoxy)-2,3-dihydro-1*H*-xanthen-4-yl)vinyl)-1-propyl-3*H*-indol-1-ium iodide (NFP-7). To a solution of the hemicyanine fluorophore (190 mg, 0.35 mmol, 1.0 eq), synthesized according to previous reports,[4-5] in DMF (3 mL) were added K_2CO_3 (96 mg, 0.70 mmol, 2 eq) and 5-(bromomethyl)-1-methyl-2-nitro-1H-imidazole (77 mg, 0.35 mmol, 1.0 eq). The mixture was stirred at room temperature for 12 h, then diluted with CH_2Cl_2 (20 mL), and washed with water (3 × 10 mL). The organic layer was dried over Na_2SO_4, filtered, and concentrated in vacuo. The resulting residue was recrystallized with CH_2Cl_2 and hexane to yield NFP-7 (69 mg, 35%) as a blue solid. ^{1}H NMR (500 MHz, CD_3OD) δ 8.80 (d, *J* = 14.9 Hz, 1H), 7.67 (dd, *J* = 7.4, 1.2 Hz, 1H), 7.58 (d, *J* = 7.9 Hz, 1H), 7.55 (dd, *J* = 7.2, 1.2 Hz, 1H), 7.52 (d, *J* = 8.7 Hz, 1H), 7.48 (dd, *J* = 7.4, 1.2 Hz, 1H), 7.38 (s, 1H), 7.35 (s, 1H), 7.21 (d, *J* = 2.4 Hz, 1H), 7.10 (dd, *J* = 8.6, 2.4 Hz, 1H), 6.57 (d, *J* = 14.9 Hz, 1H), 5.43 (s, 2H), 4.36 (t, *J* = 7.4 Hz, 2H), 4.10 (s, 3H), 2.80 (t, *J* = 5.9 Hz, 2H), 2.73 (t, *J* = 6.2 Hz, 2H), 2.01 – 1.92 (m, 4H), 1.85 (s, 6H), 1.09 (t, *J* = 7.4 Hz, 3H). ^{13}C NMR (126 MHz, CD_3OD) δ 178.39, 161.36, 161.03, 154.29, 145.94, 142.25, 141.61, 133.01, 132.98, 128.88, 128.83, 128.07, 127.89, 127.25, 122.41, 116.66, 114.42, 113.44, 112.74, 103.96, 101.69, 59.92, 50.80, 46.32, 33.68, 28.75, 26.95, 23.71, 20.92, 20.24, 10.17. HRMS calcd for $C_{33}H_{35}N_4O_4^+$ $[M]^+$ 551.2653, found 551.2639.

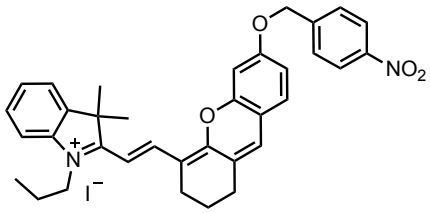

3,3-dimethyl-2-(2-(6-((4-nitrobenzyl)oxy)-2,3-dihydro-1*H*-xanthen-4-yl)vinyl)-1-propyl-3*H*-indol-1-ium iodide (NFP-8). To a solution of the hemicyanine fluorophore (200 mg, 0.37 mmol, 1.0 eq) in DMF (3 mL) were added K_2CO_3 (153 mg, 1.11 mmol, 3 eq) and 1-(bromomethyl)-4-nitrobenzene (240 mg, 1.11 mmol, 3.0 eq). The mixture was stirred at room temperature for 12 h, then diluted with CH_2Cl_2 (20 mL), and washed with water (3 × 10 mL). The organic layer was dried over Na_2SO_4, filtered, and concentrated in vacuo. The resulting residue was recrystallized with CH_2Cl_2 and hexane to yield NFP-8 (80 mg, 39%) as a blue solid. ^{1}H NMR (300 MHz, CD_3OD) δ 8.77 (d, *J* = 15.0 Hz, 1H), 8.36 – 8.27 (m, 2H), 7.77 (d, *J* = 8.5 Hz, 2H), 7.68 (d, *J* = 7.3 Hz, 1H), 7.61 – 7.44 (m, 4H), 7.39 (s, 1H), 7.13 (d, *J* = 2.4 Hz, 1H), 7.08 (dd, *J* = 8.6, 2.4 Hz, 1H), 6.54 (d, *J* = 14.9 Hz, 1H), 5.43 (s, 2H), 4.35 (t, *J* = 7.4 Hz, 2H), 2.79 (t, *J* = 6.0 Hz, 2H), 2.72 (t, *J* = 6.1 Hz, 2H), 2.01 – 1.89 (m, 4H), 1.83 (s, 6H), 1.08 (t, *J* = 7.4 Hz, 3H). ^{13}C NMR (75 MHz, CD_3OD) δ 178.21, 161.79, 161.55, 154.44, 147.83, 145.89, 144.18, 142.25, 141.72, 133.39, 129.56, 128.98, 128.92, 127.94, 127.70, 127.25, 123.51, 122.51, 116.39, 114.43, 113.66, 112.78, 103.83, 101.59, 69.18, 50.79, 46.31, 28.80, 27.04, 23.76, 21.01, 20.34, 10.30. HRMS calcd for $C_{35}H_{35}N_2O_4^+$ $[M]^+$ 547.2591, found 547.2591.

Photophysical characterization of fluorescent probes

For photophysical characterization, the fluorescent probes were dissolved in DMSO to make the stock solutions (0.5 or 1 mM). All photophysical and spectroscopic measurements were performed in phosphate buffer saline (PBS; 10 mM, pH 7.4) containing 1% DMSO. The probe stock solutions were diluted to 5 or 10 μM as the testing solutions with PBS. NADH (Sigma) and NTR (Sigma) were dissolved in PBS and added into the probe solutions at indicated concentrations. Absorption spectra were recorded on a Techcomp UV-1000 UV-Visible spectrophotometer. Fluorescence spectra were recorded on a Hitachi F-4600 fluorescence spectrophotometer or a Biotek Cytation 5 Multi-Mode Reader. For measurements on Hitachi F-4600, samples were in 1 cm × 1 cm quartz cuvettes.

To test the absorption and fluorescence responses of fluorescent probes toward NTR, the probe solutions (5 or 10 μM final concentration) were incubated with NTR at different concentrations in the presence of NADH (500 μM unless stated) at 37 °C for 10–60 min. The volume changes after addition of the NTR solutions were less than 1%. For kinetic analysis, the fluorescence intensities of fluorescent probes were monitored with time immediately after addition of the NTR solution. Fluorescence intensities of NFP-1–6 were measured at 585 nm with excitation at 550 nm. Fluorescence intensities of NFP-7–8 were measured at 705 nm with excitation at 670 nm.

For selectivity assays, the probe solutions in PBS (10 μM) were treated with the analyte of interest as described above at 37 °C for 60 min. Potential interfering species were obtained from commercial sources, and their concentrations are as follows: KCl (50 mM), NaCl (50 mM), $CaCl_2$ (50 mM), tyrosine (Tyr, 1 mM), glycine (Gly, 1 mM), tryptophan (Trp, 1 mM), methionine (Met, 1 mM), glutamic acid (Glu, 1 mM), glucose (10 mM), lysozyme (0.1 mg/mL), GSH (10 mM), DTT (1 mM), H_2O_2 (1 mM), KO_2 (1 mM), Na_2SO_3 (1 mM), and NaClO (10 μM).

For estimation of probe detection limit, a linear correlation between the fluorescence intensity of probe and NTR concentration was firstly investigated and the equation of linear regression was thus obtained. The detection limit of probe was calculated by $3\sigma/k$, where σ is the standard deviation of probe fluorescence intensity before reaction with NTR (n = 10) and k is the slope of linear equation.

For calculation of K_m and V_{max}, fluorescence response kinetics were examined for probes (NFP-7–8) of different concentrations (2.5–20 μM) in the presence of NTR (0.1 μg/mL for NFP-7 and 1 μg/mL for NFP-8) and NADH (500 μM) at 37 °C. The initial rate of reaction between the probe and NTR was measured by monitoring the fluorescence increase over time. The reaction rate was then calculated using the fluorescence calibration curve of released hemicyanine fluorophore. A Lineweaver−Burk double-reciprocal plot of 1/rate versus 1/concentration was thus generated, and the Michaelis–Menten constant (K_m) and maximal rate (V_{max}) were calculated based on the Lineweaver-Burk equation: $1/V = 1/V_{max} + K_m/V_{max} \cdot 1/[probe]$, where V is the initial reaction rate, [probe] is the probe concentration, K_m is the Michaelis constant, and V_{max} is the maximal reaction rate.

LC-MS analysis on reaction of NFP-7 with NTR

To a solution of NFP-7 (200 μM) and NADH (1 mM) in PBS was added the NTR stock solution to a final concentration of 1 μg/mL. The mixture was incubated at 37 °C for 5 min and then directly analyzed by LC-MS on a Q Exactive Focus LC-MS/MS System. The UV detector was set at 254 nm and 600 nm. Samples were eluted from a Hypersil GOLD VANQUISH C18 UHPLC column (100 × 2.1 mm, 1.9 μm) with a linear gradient from 10% acetonitrile/90% water containing 0.1 % FA to 95% acetonitrile/5% water containing 0.1 % FA in 8 min at a flow rate of 0.28 mL/min. An ESI ionization source was used for MS analysis.

Docking calculations

The molecular docking calculations between NFP-1–5 and NTR were performed using LeDock software (http://www.lephar.com).[6-7] The chemical structures of NFP-1–5 were generated and optimized in Chem3D (PerkinElmer). NTR structure was obtained from PDB database (PDB ID: 4DN2). The docking calculation results were visualized with PyMOL software.

Cell culture

HepG2 and HeLa cells were purchased from the American Type Culture Collection (ATCC) and grown in Dulbecco's Modified Eagle's Medium (DMEM; Corning, 10-013-CVR) supplemented with 10% fetal bovine serum (FBS; Corning, 35-076-CV) at 37 °C in a humidified incubator with an atmosphere of 5% CO_2.

Confocal fluorescence imaging in live cells

HepG2 and HeLa cells were plated on 35-mm cover-slip dishes (MatTek, P35G-1.5-10-C) and allowed to adhere for overnight. The cells were incubated with NFP-7 or NFP-8 (5 μM) in DMEM supplemented with 10% FBS under normoxic (20% O_2) or different hypoxia conditions (10% or 1% O_2) for 5 h. The hypoxia conditions were generated with an AnaeroPack (Mitsubishi Gas Corp.). Then the cells were washed with cold PBS three times and imaged on an A1R confocal fluorescence microscope (Nikon) with a 60 x oil immersion objective lens. The fluorescence signals of NFP-7–8 were collected between wavelengths of 663 and 738 nm, with excitation at 640 nm. For dicoumarin treatment, cells were treated with dicoumarin (0.2 mM) together with the probe.

Image quantification and analysis were performed with ImageJ software (NIH). At least three fields of view per well were randomly selected for every fluorescence imaging experiment. The fluorescence intensity of every image was quantified in ImageJ and averaged to be the mean fluorescence intensity of the well. For each conditions, multiple wells (reported as *n*) were analyzed. The mean fluorescence intensities of these wells were averaged and grouped for statistical analysis.

MTT assay

The cytotoxicity of NFP-7 in HepG2 and HeLa cells was measured using methyl thiazolyl tetrazolium (MTT) assay. Briefly, about 1 x 10^4 cells per well were seeded into 96-well cell-culture plates and cultured for 24 h. Then the cells were treated with NFP-7 at different concentrations (100 μL/ well). After incubation for 12 h at 37 °C/5% CO_2, 10 μL of MTT solution

(Beyotime, C0009; 5 mg/mL) was added into each well and incubated with the cells for 4 h at 37 °C. Then 100 μL of Formazan solvent (Beyotime, C0009) was added into each well. The plates were further incubated for 4 h at 37 °C and the absorbance of each well was measured at 570 nm with a Biotek Epoch microplate spectrophotometer. The cell viability (%) was calculated by the following equation: viability (%) = A/A_0 x 100, where A is the absorbance of cells with probe treatment and A_0 is the absorbance of cells without probe treatment.

In vivo fluorescence imaging in a murine tumor model

Animal experimental protocol was approved by Peking University Shenzhen Graduate School Institutional Animal Care and Ethical Committee. Murine tumor model was generated by Beijing Vital River Laboratory Animal Technology Co., Ltd. Briefly, about 1 x 10^6 HepG2 cells were grafted into a nude C57BL/6J mouse. Tumors with diameters of about 7.5 and 12 mm were used in this study.

In vivo fluorescence imaging was performed using the IVIS Spectrum *in vivo* imaging system (PerkinElmer). Briefly, the mice were anesthetized with inhalation of 2% isoflurane for 30 s in an anaerobic box before imaging. After an intratumor injection of NFP-7 (50 μM) in 0.1 mL saline, the mice were placed in the IVIS Spectrum imaging system for *in vivo* fluorescence imaging with excitation and emission at 675 nm and 720 ± 10 nm, respectively. For dicoumarin treatment, 100 μL of dicoumarin (1 mM) in saline was injected into the tumor before injection of the probe solution.

Reference

1. Tercel, M.; Stevenson, R. J.; Lu, G.-L.; Stribbling, S. M.; Wilson, W. R.; Tatnell, M. A.; Marnane, R. N.; Mountjoy, K. G.; Denny, W. A., Weight loss effects of quaternary salts of 5-amino-1-(chloromethyl)-1,2-dihydro-3H-benz[e]indoles; structure–activity relationships. *Biorg. Med. Chem.* **2012,** *20* (2), 734-749.
2. O'Connor, L. J.; Cazares-Körner, C.; Saha, J.; Evans, C. N. G.; Stratford, M. R. L.; Hammond, E. M.; Conway, S. J., Design, synthesis and evaluation of molecularly targeted hypoxia-activated prodrugs. *Nat. Protoc.* **2016,** *11* (4), 781-794.
3. Bielec, B.; Schueffl, H.; Terenzi, A.; Berger, W.; Heffeter, P.; Keppler, B. K.; Kowol, C. R., Development and biological investigations of hypoxia-sensitive prodrugs of the tyrosine kinase inhibitor crizotinib. *Bioorg. Chem.* **2020,** *99*, 103778.
4. Yuan, L.; Lin, W.; Zhao, S.; Gao, W.; Chen, B.; He, L.; Zhu, S., A Unique Approach to Development of Near-Infrared Fluorescent Sensors for in Vivo Imaging. *J. Am. Chem. Soc.* **2012,** *134* (32), 13510-13523.
5. Zhang, C.; Zhai, B.-B.; Peng, T.; Zhong, Z.; Xu, L.; Zhang, Q.-Z.; Li, L.-Y.; Yi, L.; Xi, Z., Design and synthesis of near-infrared fluorescence-enhancement probes for the cancer-specific enzyme hNQO1. *Dyes Pigm.* **2017,** *143*, 245-251.
6. Zhang, N.; Zhao, H., Enriching screening libraries with bioactive fragment space. *Bioorg. Med. Chem. Lett.* **2016,** *26* (15), 3594-3597.
7. Wang, Z.; Sun, H.; Yao, X.; Li, D.; Xu, L.; Li, Y.; Tian, S.; Hou, T., Comprehensive evaluation of ten docking programs on a diverse set of protein–ligand complexes: the prediction accuracy of sampling power and scoring power. *Phys. Chem. Chem. Phys.* **2016,** *18* (18), 12964-12975.

NMR spectra

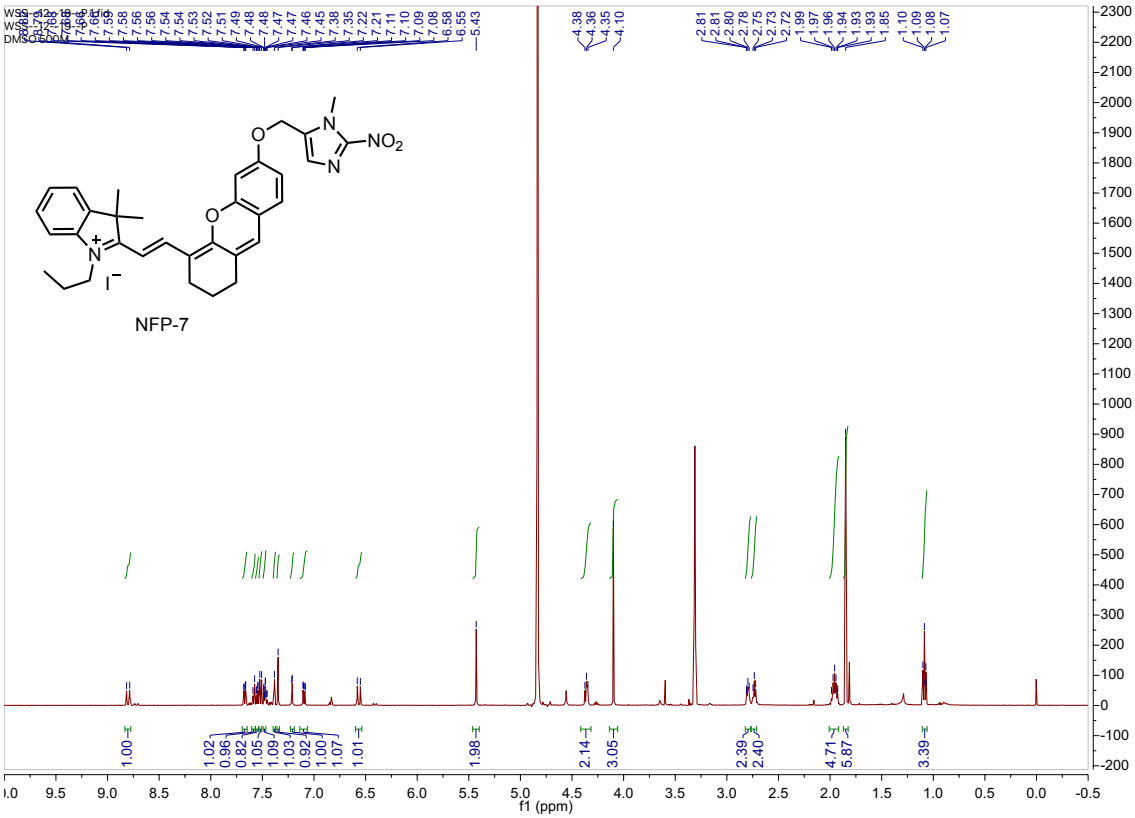

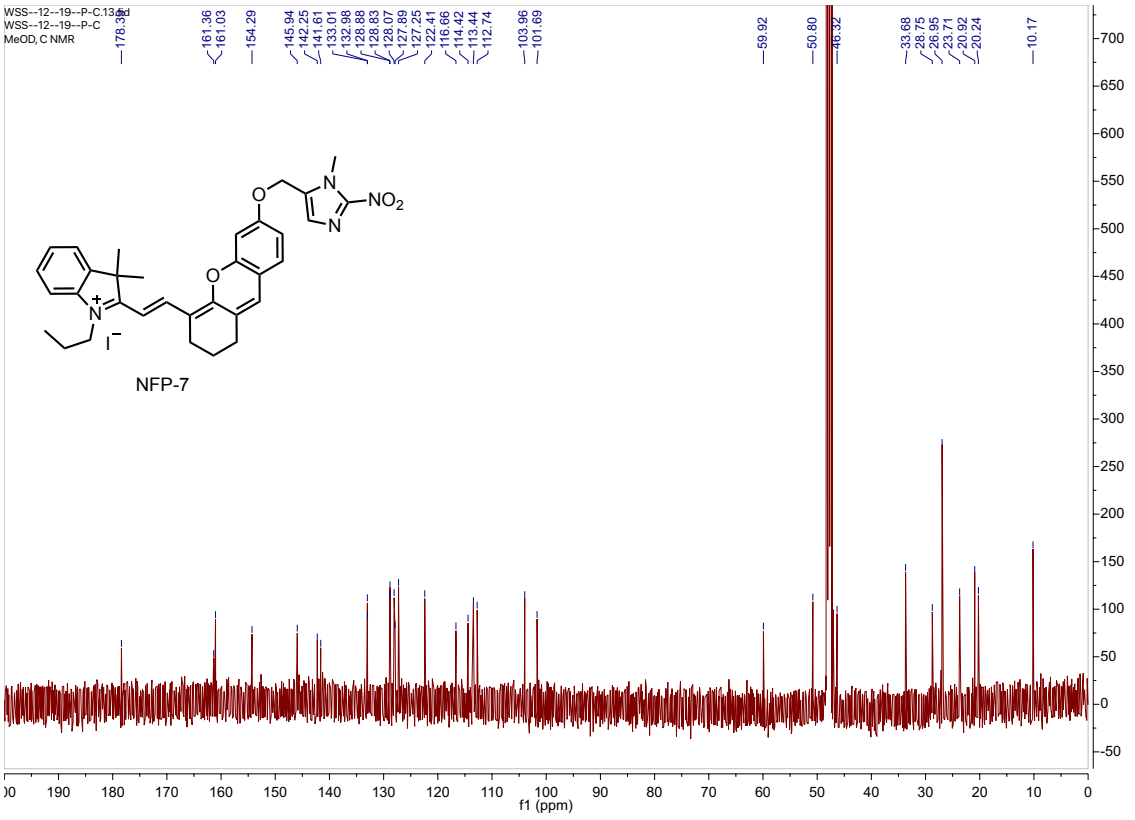

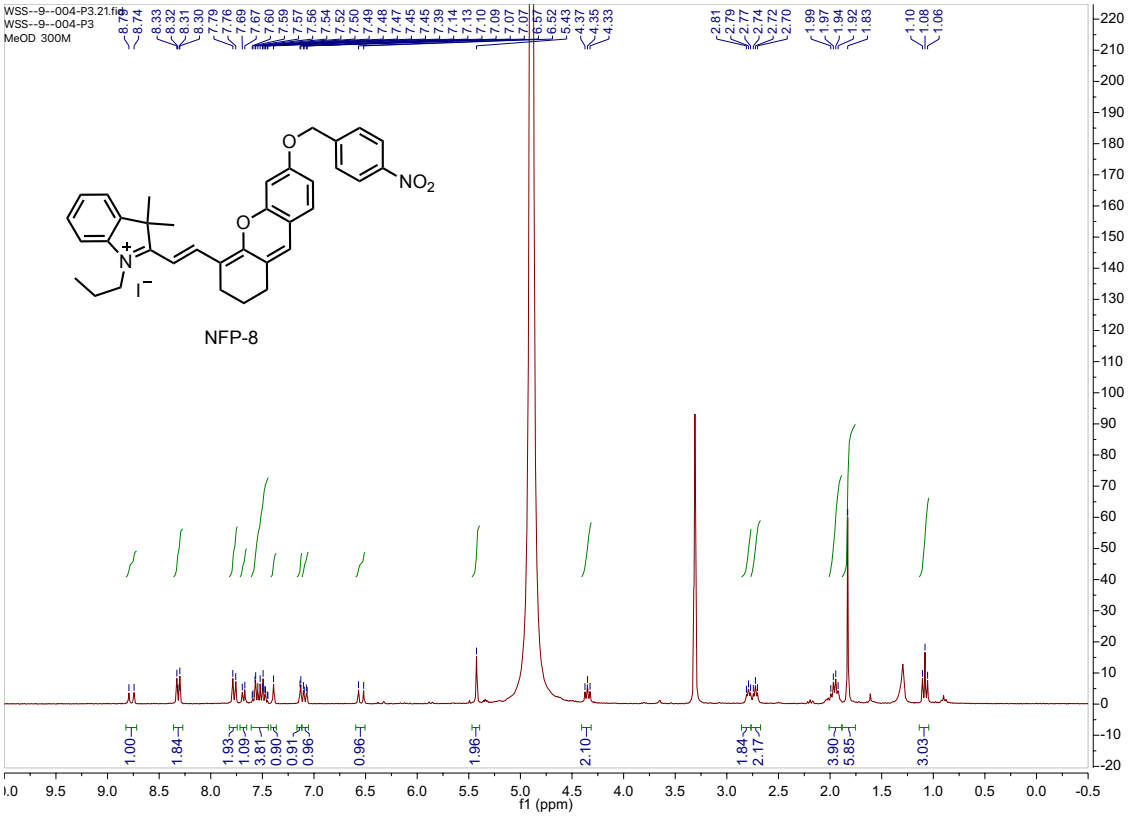
WSS--9---004-P3.21.fid
WSS--9---004-P3
MeOD 300M
NFP-8
f1 (ppm)

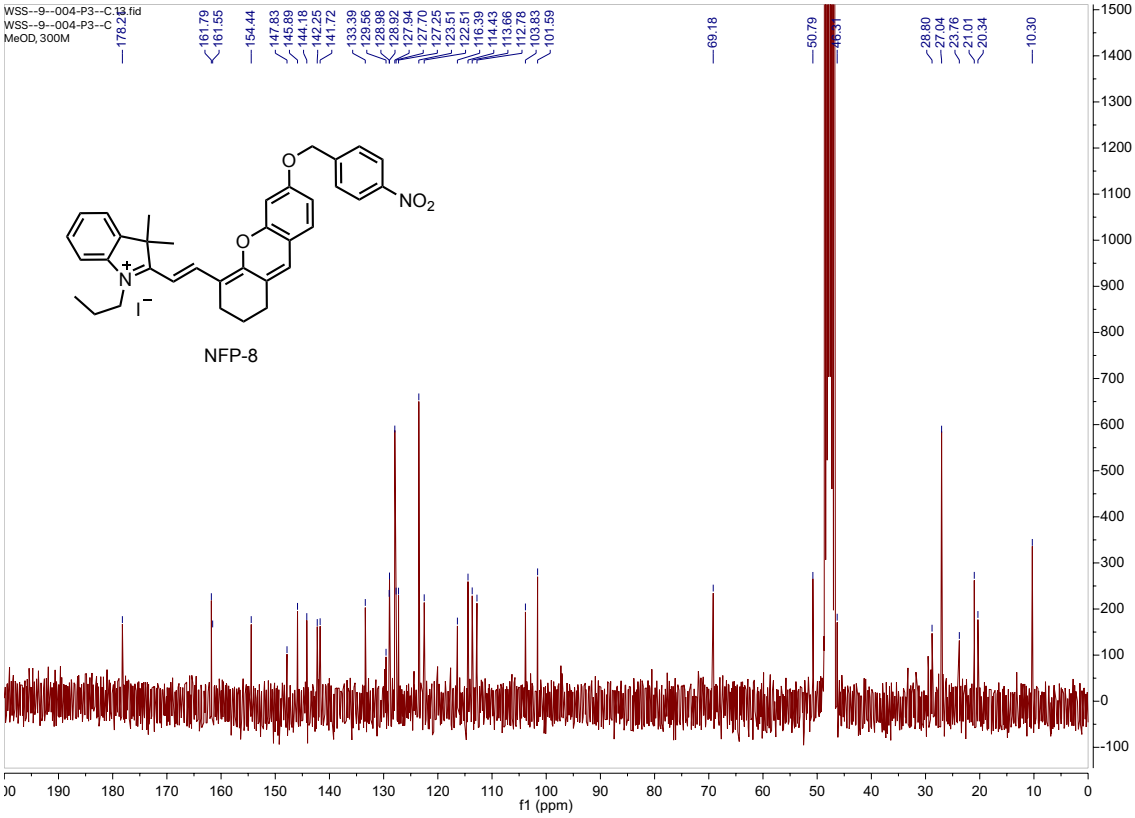
WSS--9---004-P3--C 13.fid
WSS--9---004-P3--C
MeOD, 300M
NFP-8
f1 (ppm)